ZOOLOGICAL SCIENCE **22**: 735–742 (2005)

Amphipathic α-Helix Mediates the Heterodimerization of Soluble Guanylyl Cyclase

Takumi Shiga and Norio Suzuki*

Division of Biological Sciences, Graduate School of Science, Hokkaido University, Sapporo 060-0810, Japan

ABSTRACT—Soluble guanylyl cyclase (soluble GC) is an enzyme consisting of α and β subunits and catalyzes the conversion of GTP to cGMP. The formation of the heterodimer is essential for the activity of soluble GC. Each subunit of soluble GC has been shown to comprize three functionally different parts: a C-terminal catalytic domain, a central dimerization domain, and an N-terminal regulatory domain. The central dimerization domain of the β_1 subunit, which contains an N-terminal binding site (NBS) and a C-terminal binding site (CBS), has been postulated to be responsible for the formation of α/β heterodimer. In this study, we analyzed heterodimerization by the pull-down assay using the affinity between a histidine tag and Ni^{2+} Sepharose after co-expression of various N- and C-terminally truncated FLAG-tagged mutants of the α_1 subunit and the histidine-tagged wild type of the β_1 subunit in the vaculovirus/Sf9 system, and demonstrated that the CBS-like sequence of the α_1 subunit is critical for the formation of the heterodimer with the β_1 subunit and the NBS-like sequence of the α_1 subunit is essential for the formation of the enzymatically active heterodimer, although this particular sequence was not involved in heterodimerization. The analysis of the secondary structure of the α_1 subunit predicted the existence of an amphipathic α-helix in residues 431–464. Experiments with site-directed α_1 subunit mutant proteins demonstrated that the amphipathicity of the α-helix is important for the formation of the heterodimer, and Leu^{463} in the α-helix region plays a critical role in the formation of a properly arranged active center in the dimer.

Key words: soluble guanylyl cyclase, cGMP, heterodimer, dimerization region, recombinant protein, pull-down assay, amphipathic α-helix, secondary structure

INTRODUCTION

Both the soluble and membrane forms of guanylyl cyclases (GCs) catalyze the conversion of GTP to cGMP, which is a ubiquitous second messenger in intracellular signaling cascades and responsible for a wide variety of physiological responses (Drewett and Garbers, 1994; Garbers and Lowe, 1994; Garbers *et al.*, 1994). Soluble GC is a heterodimer consisting of α and β subunits, and contains a prosthetic ferrous heme group to which nitric oxide (NO) binds with high affinity. The formation of an NO-heme complex and the subsequent conformational change in the heterodimer are responsible for the up to 200-fold increase in the catalytic rate of this enzyme (Gerzer *et al.*, 1981; Humbert *et al.*, 1990; Stone and Marletta, 1994). In mammals, cDNAs for four soluble GC subunits (α_1, α_2, β_1, and β_2) have been isolated from various tissues (Koesling *et al.*, 1988; Koesling *et al.*, 1990; Yuen *et al.*, 1990; Harteneck *et al.*, 1991). Both the α_1/β_1 and α_2/β_1 heterodimers have been shown to be enzymatically active when formed in an *in vitro* expression system (Russwurm *et al.*, 1991). A single expression of either one of the subunits has been shown to yield an α_1/α_1- or a β_1/β_1-homodimer, although both homodimers were catalytically inactive (Zabel *et al.*, 1999). In previous studies, we have isolated and characterized the cDNA and genomic DNA clones encoding the soluble GC subunits, *OlGCS-*α_1 and *OlGCS-*β_1, both of which are aligned in tandem on the genome of the medaka fish *Oryzias latipes* (Mikami *et al.*, 1998, 1999). We recently demonstrated that the medaka fish contains another type of a soluble GC subunit gene, *OlGCS-*α_2, which is located on a different linkage group of *OlGCS-*α_1 and *OlGCS-*β_1 (Yao *et al.*, 2003).

Each subunit of soluble GC can be divided functionally into three parts: a C-terminal catalytic domain, a central region commonly referred to as the dimerization domain, and an N-terminal regulatory domain participating in heme binding (Koesling, 1999). The His^{105} site in residue of the β_1 subunit has been identified as the proximal heme ligand site (Wedel *et al.*, 1994; Zhao *et al.*, 1998; Foerster *et al.*, 1996).

* Corresponding author. Phone: +81-11-706-4908;
Fax : +81-11-706-4461;
E-mail: norio-s@sci.hokudai.ac.jp

The C-terminal catalytic domain is highly conserved among various soluble GC subunits and is thought to be responsible for catalysis, as based on its homology with a related domain of adenylyl cyclase (Koesling, 1999). Dimerization has been attributed to the central region of the soluble GC subunits; this attribution is primarily based on studies of peptide receptor/membrane GCs (Wilson and Chinkers, 1996). It was recently demonstrated that the dimerization domain of the β_1 subunit consists of 205 amino acid residues across the regulatory and central regions and contains discontinuous sequences consisting of 41 amino acid residues (N-terminal binding site: NBS) and 30 amino acid residues (C-terminal binding site: CBS), respectively, that facilitate the binding of the β_1 subunit to the α_1 subunit (Zhou *et al.*, 2004). However, the function of the N-terminal portion of the α_1 subunit has remained unknown, although several studies have shown that the N-terminal portion of the α_1 subunit is critical for heme-binding (Wedel *et al.*, 1995); moreover, it was shown that deletion of the 259 N-terminal amino acids from the α_1 subunit exerted no effect whatsoever on the properties of the enzyme, and amino acids 259–364 of the α_1 subunit represent an important functional domain for the transduction of the NO-activation signal (Koglin and Behrends, 2003). Although soluble GC has not yet been crystallized for X-ray diffraction analysis, it is predicted that its catalytic domain resembles that of the class III adenylyl cyclases (Tucker *et al*, 1998; Sunahara *et al.*, 1998). Structural analysis of the catalytic core of the adenylyl cyclases has demonstrated an antiparallel orientation of the two catalytic domains (C_1 and C_2) with two pockets, the formation of each of which involves both of the catalytic domains (Zhang *et al.*, 1997; Tesmer *et al.*, 1997).

To investigate the dimerization region of the α_1 subunit, we generated several recombinant soluble GC subunits in an expression system with Sf9 cells and performed a pull-down assay using the affinity between the histidine tag and Ni^{2+} Sepharose. Here, we report that the NBS-like sequence of OlGCS-α_1 is not involved in the formation of the heterodimer with OlGCS-β_1, but it does appear to play an important role in the formation of the enzymatically active heterodimer. We also report here that the CBS-like sequence of OlGCS-α_1 is involved in the formation of a heterodimer with OlGCS-β_1 and that the amphipathic α-helix of OlGCS-α_1 is critical for the formation of a heterodimer with OlGCS-β_1.

MATERIALS AND METHODS

Construction of a plasmid for histidine-tagged OlGCS-β_1-full length protein (FL_{HT})

Total RNA was isolated from the adult brain of *O. latipes* by the acid/guanidinium/thiocyanate/phenol/chloroform extraction method (Chomczynski and Sacchi, 1987). Total RNA (5 μg) was used as the template to synthesize the first strand cDNA using an oligo(dT) primer, and the Super Script II preamplification system was used according to the manufacturer's protocol for first-strand cDNA synthesis (Gibco BRL, Tokyo, Japan). To obtain a C-terminal histidine-tagged OlGCS-β_1-full length protein (OlGCS-β_1-FL_{HT}), we designed the following primers: 5'-GTG GAT CCA TGT ATG GTT TTG TGA AT-3' and 5'-CGC GTC GAC TTA GTG ATG GTG ATG GTG ATG TGC CTT GTC AGC GTC GCT GC-3'. PCR was performed using *Ex Taq* polymerase (TaKaRa, Otsu, Japan) according to manufacturer's protocol with the following PCR conditions: 30 cycles of 30 sec at 94°C, 30 sec at 50°C, 4 min at 72°C, and a final extension of 5 min at 72°C. The cDNA fragment amplified by the PCR was purified and subcloned into the plasmid vector pBluescript II KS(–) (Stratagene, La Jolla, CA, USA). A *Bam*HI/*Sal*I insert from the *OlGCS-β_1* clone in the pBluescript II KS(–) vector was ligated into the *Bam*HI/*Sal*I cut pFASTBAC1 vector (Invitrogen Japan K. K., Tokyo, Japan).

Construction of plasmids for FLAG-tagged OlGCS-α_1-full length protein (FL_{FLAG}) and its truncated mutant proteins

To obtain a C-terminal FLAG-tagged OlGCS-α_1-full length protein (OlGCS-α_1-FL_{FLAG}) and several N-terminal and C-terminal deletion mutant proteins of OlGCS-α_1, we performed PCR using an *OlGCS-α_1* clone in pBluescript II KS(–) as a template. PCR was performed with various primers using *Pfu* polymerase (TaKaRa) according to the manufacturer's protocol (Table 1). The following PCR parameters were used: 30 cycles of 30 sec at 94°C, 30 sec at each annealing temperature shown in Table 1, and 2 min at 72°C, with a final extension of 5 min at 72°C. Each PCR product was purified and digested by *Spe*I and *Xho*I. The resulting *Spe*I/*Xho*I-cut PCR product was subcloned into the pFASTBAC1 vector.

Construction of plasmids for C-terminal FLAG-tagged site-directed OlGCS-α_1 mutant proteins

Mutagenesis of *OlGCS-α_1* was performed using the following primers: 5'-GCC CAG GAT GGC AAG AAG AAG CG-3' for L434K, 5'-GGC AGC CAA GGA AAA CGC TCA CC-3' for L445K, 5'-CGC TCA CCA AGC GAA GGA GGA GG-3' for L453K, and 5'-GAT CTT AAG TTT TCC ATT TTC CC-3' for L463K. As a template for the mutagenesis, we used the pFASTBAC1 vector containing the C-terminal FLAG-tagged intact *OlGCS-α_1*-full length sequence. The mutagenesis was performed by the site-directed and semi-random mutagenesis procedure (Sawano and Miyawaki, 2000).

Generation of recombinant baculovirus

The accuracy of the sequences of all clones was confirmed by DNA sequencing. Each sequence was confirmed by the dideoxy chain termination procedure (Sanger *et al.*, 1992) with an ABI PRISM 3100 Genetic Analyzer (Applied Biosystems, Osaka, Japan) and analyzed with GENETYX-MAC/version 7.2.0 software (Software Development, Tokyo, Japan). Recombinant baculovirus of each respective clone was generated according to a BAC-TO-BAC Baculovirus Expression System (Invitrogen Japan K. K.).

Sf9 cell culture, expression of recombinant soluble GC subunit constructs and mutants, and cytosol preparation

Sf9 cells were cultured in SF-900 II serum-free medium supplemented with 50 μg/ml streptomycin, 50 U/ml penicillin, and 20% fetal bovine serum (FBS). Spinner cultures were grown to a cell density of 3.0×10^6 cells/ml and then the cultures were diluted to 2.0×10^6 cells/ml in a tissue culture flask. Ten ml of the culture medium containing Sf9 cells (2.0×10^6 cells/ml) were infected with each virus stock of OlGCS-α_1 or were co-infected with OlGCS-β_1-FL_{HT}-containing virus (ratio 1:1), and then the samples were cultured for an additional 4 days at 37°C. All subsequent experiments were carried out at 4°C. The cells were harvested by centrifugation at 1,000 g for 5 min. The resulting pellet was washed in 1 ml of ice-cold phosphate-buffered saline (PBS), pH 6.2, and then was resuspended in 500 μl of an ice-cold lysis buffer for the pull-down assay (50 mM phosphate buffer, pH 7.2, containing 100 mM NaCl, 10% glycerol, and 0.1% protease inhibitor mixture in DMSO solution)

Table 1. Primers and the annealing temperatures used for the construction of plasmids for OlGCS-α_1-FL_{FLAG} and its truncated mutants.

	Sequence[s] of primers	Annealing temperature
a1-FLFLAG		44°C
a1start-SpeI	5'-ACTAGTATGTTCTGCGGCCAAGTTGAA-3'	
a1endFLAG*XhoI	5'-CTCGAGTCACTTGTCATCGTCGTCCTTGTAGTCTTTTTTTGTAAGTTTTGACA-3'	
a1[280-678]FLAG		44°C
a1-dN279	5'-ACTAGTATGACCTCTGCTGGAACGCTCCC-3'	
a1endFLAG*XhoI	5'-CTCGAGTCACTTGTCATCGTCGTCCTTGTAGTCTTTTTTTGTAAGTTTTGACA-3'	
a1[322-678]FLAG		44°C
a1-dN321	5'-ACTAGTATGGGACTTAGAAGGTCTCCCAC-3'	
a1endFLAG*XhoI	5'-CTCGAGTCACTTGTCATCGTCGTCCTTGTAGTCTTTTTTTGTAAGTTTTGACA-3'	
a1[1-477]		54°C
a1start-SpeI	5'-ACTAGTATGTTCTGCGGCCAAGTTGAA-3'	
a1-dC477	5'-CTCGAGTCACTTGTCATCGTCGTCCTTGTAGTCCTGCCACAGCTGCTGGGCCA-3'	
a1[1-448]		54°C
a1start-SpeI	5'-ACTAGTATGTTCTGCGGCCAAGTTGAA-3'	
a1-dC448	5'-CTCGAGTCACTTGTCATCGTCGTCCTTGTAGTCGTTTTCCAAGGCTGCCTTGG-3'	

(Wako, Osaka, Japan) or the pellet was resuspended in lysis buffer to detect GC activity (20 mM Tris-HCl, pH 6.8, 90 mM NaCl, 10% glycerol, and 0.1% protease inhibitor mixture-dimethylsulfoxide (DMSO) solution). The suspension was sonicated and then centrifuged at 15,000 g for 20 min, and the resulting supernatant fraction was collected and used for subsequent experiments.

Determination of protein concentration, Western blot analysis, and pull-down assay

The protein concentration was determined by the BCA method using BCA protein assay reagent (PIERCE, Rockford, IL, USA). Before each pull-down assay, sodium dodecyl sulfate-polyacrylamide gel electrophoresis (SDS-PAGE) and Western blotting were used to confirm that similar levels of protein were expressed in each lysate. The cell lysates were subjected to SDS-PAGE on a 10% polyacrylamide gel and transferred to PVDF membranes, which were blocked with 2% dry milk in TPBS (PBS, pH 7.4, containing 0.1% Tween 20) for 15 min at room temperature, rinsed, and incubated overnight at 4°C with anti-His-Tag antibody (MBL, Nagoya, Japan) or ANTI-FLAG M2 monoclonal antibody-alkaline phosphatase conjugate (SIGMA, Saint Louis, MO, USA) in TPBS containing 0.2% dry milk. Subsequently, the anti-His-Tag antibody-treated membrane was incubated with secondary antibody for 1 h at room temperature. Immunoreacted proteins were detected using ready-to use CDP-Star (Roche, Tokyo, Japan) or Western blot detection reagents (Amersham). The density of each band was determined by scanning the images using Scion Image Beta 4.0.2 (Scion corporation, Frederick, MD, USA). The lysis buffer for the pull-down assay containing 500 μg protein was incubated overnight at 4°C with 150 μl of chelating Sepharose (Amersham Pharmacia Biotech, Tokyo, Japan), which was preincubated in a total volume of 600 μl containing 75 μl of 0.2 M $NiCl_2$ for 5 min according to the manufacturer's protocol. Each sample was washed 3 times with 750 μl of the ice-cold lysis buffer used for the pull-down assay, and then the samples were washed 3 times with 300 μl of the ice-cold lysis buffer used for the pull-down assay, to which 15 mM imidazole had been added. The proteins were then eluted with the ice-cold lysis buffer used for the pull-down assay, which also contained 150 mM imidazole. The eluted proteins were subjected to SDS-PAGE and Western blot analysis, as described above.

Assay of GC activity

Before the assay of GC activity was performed, SDS-PAGE and Western blot analysis were carried out in order to confirm that similar levels of protein were expressed in each cytosolic fraction. The GC activity of the cytosolic fraction (50 μg protein/assay tube) was determined in a total volume of 250 μl by incubation for 15 min at 37°C in an assay solution (50 mM Tris-HCl, pH 7.5, 4 mM $MgCl_2$, 0.5 mM 3-isobutyl-1-methylxanthine (IBMX), 7.5 mM creatine phosphate, 25 U/ml creatine phosphokinase, and 1 mM GTP) with or without 1 mM sodium nitroprusside dihydrate (SNP). The reaction was stopped by boiling the sample for 3 min, and then each assay tube was centrifuged at 15,000 g for 10 min. The amount of cGMP in the supernatant was determined by use of a cGMP enzyme immunoassay system (Amersham Biosciences, Tokyo, Japan).

RESULTS AND DISCUSSION

Identification of N-terminal binding site (NBS) and C-terminal binding site (CBS) of OlGCS-α_1

To assign the putative NBS- and CBS-like sequences of OlGCS-α_1, the amino acid sequence of OlGCS-α_1 was aligned with that of rat soluble GC-α_1. The sequence identities of the NBS-like sequence of OlGCS-α_1 at positions 280–321 and the CBS-like sequence of OlGCS-α_1 at positions 448–477 to those of the corresponding rat soluble GC-α_1 were 45.2 and 90%, respectively. To define the binding ability of the NBS-like sequence of OlGCS-α_1 and the CBS-like sequence of OlGCS-α_1 to OlGCS-β_1, we generated FLAG-tagged N-terminal deletion mutants and C-terminal deletion mutants of OlGCS-α_1 (Fig. 1), and both types of mutant were separately expressed or co-expressed with the OlGCS-β_1-FL_{HT} in Sf9 cells.

To examine the binding ability of the NBS-like sequence to OlGCS-β_1-FL_{HT}, we performed a pull-down assay (Fig. 2A). OlGCS-α_1-FL_{FLAG}, OlGCS-α_1[280-678]$_{FLAG}$, and OlGCS-

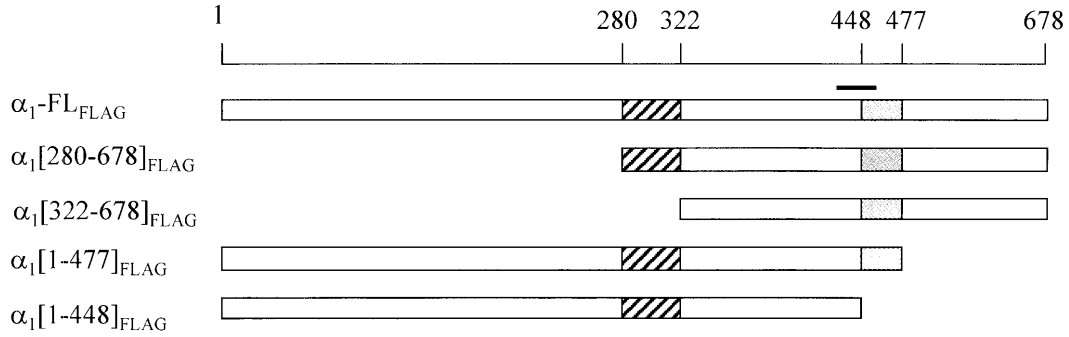

Fig. 1. Schematic representation of various OlGCS-α_1 constructs. The NBS-like sequence (280–321) is indicated by hatched boxes and the CBS-like sequence is indicated by shaded boxes. Numbers denote the relative positions of the amino acids. The boldfaced line indicates the predicted amphipathic α-helix region.

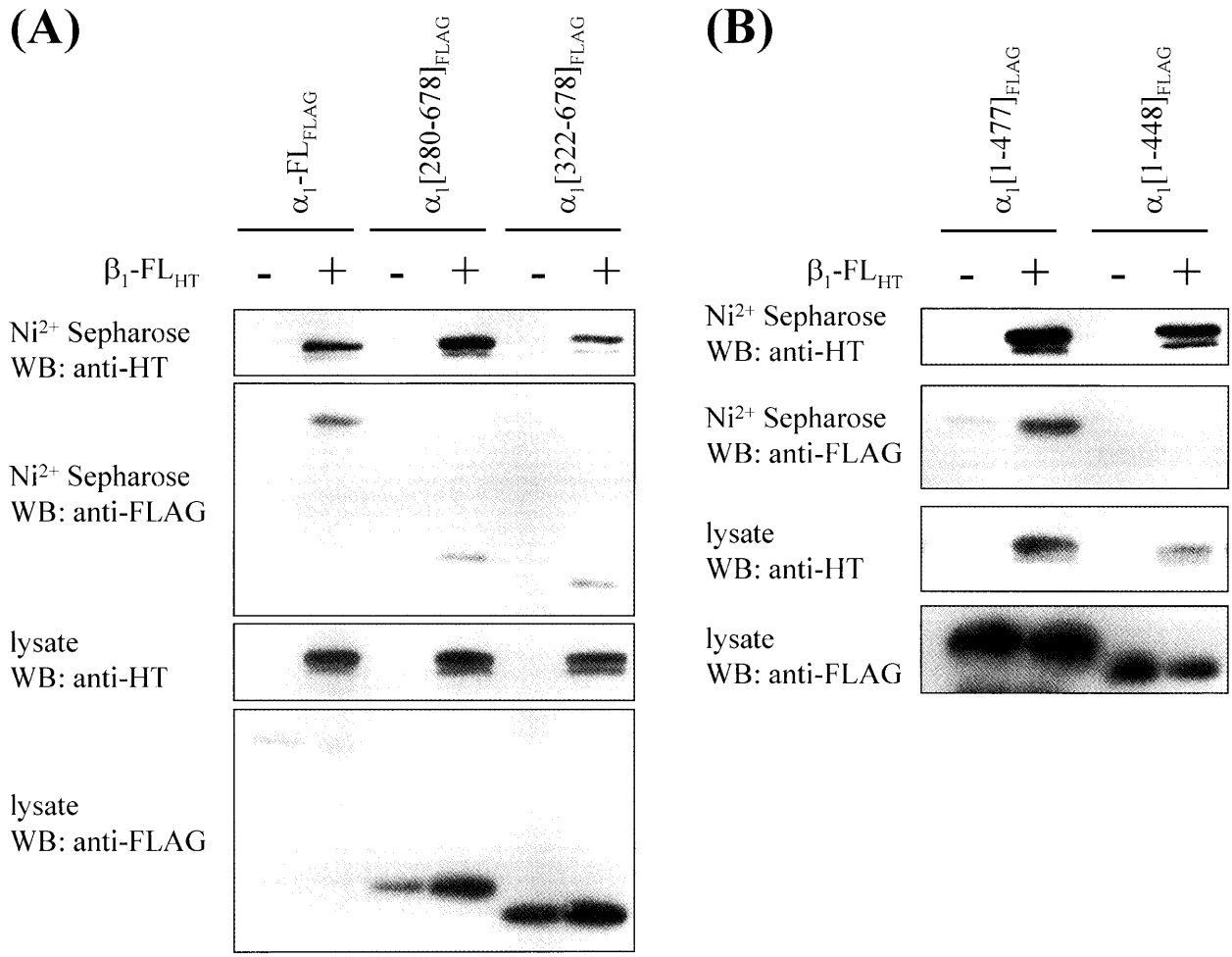

Fig. 2. Pull-down assay of the NBS-like and the CBS-like sequences. Sf9 cells were infected with baculovirus containing its N-terminal deletion mutants of *OlGCS-α_1-FL$_{FLAG}$* (A), or the C-terminal deletion mutants of *OlGCS-α_1-FL$_{FLAG}$* (B), with or without *OlGCS-β_1-FL$_{HT}$*. Almost equal amounts of OlGCS-β_1-FL$_{HT}$ were detected in the Ni^{2+} Sepharose-binding fraction by Western blot (WB) analysis using anti-His-Tag (anti-HT) antibody (top). The Ni^{2+} Sepharose-binding fraction was analyzed by Western blotting with anti-FLAG antibody (upper middle). To confirm the protein expression levels in the lysate, Western blotting was performed using anti-HT antibody or anti-FLAG antibody (lower middle and bottom, respectively). Similar results were obtained from two independent experiments.

α_1[322-678]$_{FLAG}$ were unable to bind to Ni^{2+} Sepharose when each construct was expressed without *OlGCS-β_1-FL$_{HT}$*. Both OlGCS-α_1[280-678]$_{FLAG}$ and OlGCS-α_1[322-678]$_{FLAG}$ fully retained their ability to bind to OlGCS-β_1-FL$_{HT}$, judging from the result that each OlGCS-α_1 N-terminal deletion protein was detected in the Ni^{2+} Sepharose-binding fraction. This finding suggests that the NBS-like sequence of OlGCS-α_1 (280–321) is not involved in the heterodimerization with OlGCS-β_1.

We then examined the binding ability of the C-terminal deletion mutant proteins of OlGCS-α_1 to OlGCS-β_1. Co-expression of *OlGCS-α_1[1-448]$_{FLAG}$* or *OlGCS-α_1[1-477]$_{FLAG}$* with *OlGCS-β_1-FL$_{HT}$* was followed by pull-down assay and Western blot analysis. As shown in Fig. 2B, OlGCS-α_1[1-448]$_{FLAG}$ did not exhibit any binding ability to OlGCS-β_1-FL$_{HT}$, and no protein band was detected in the Ni^{2+} Sepharose-binding fraction of α_1[1–448]$_{FLAG}$/β_1-FL$_{HT}$, as observed by anti-FLAG antibody. Conversely, OlGCS-α_1[1-477]$_{FLAG}$ did bind to OlGCS-β_1-FL$_{HT}$, suggesting that the CBS-like sequence of OlGCS-α_1 contains the structural elements that mediate heterodimerization with OlGCS-β_1-FL$_{HT}$.

To examine the GC activity of the N-terminal deletion mutant proteins of OlGCS-α_1, *OlGCS-α_1-FL$_{FLAG}$*, *OlGCS-α_1[280–678]$_{FLAG}$*, or *OlGCS-α_1[322–678]$_{FLAG}$* was co-expressed with *OlGCS-β_1-FL$_{HT}$* in Sf9 cells, and the GC activity of the cytosolic fraction of each sample was measured. As shown in Fig. 3, α_1[280–678]$_{FLAG}$/β_1-FL$_{HT}$ showed basal and SNP-stimulated GC activity to almost the same extent as that of the control soluble GC (α_1-FL$_{FLAG}$/β_1-FL$_{HT}$), although α_1-[322–678]$_{FLAG}$/β_1-FL$_{HT}$ did not exhibit any GC activity with or without SNP. Therefore, we predicted that the NBS-like sequence of OlGCS-α_1 (amino acids 280–321) plays an important role in the correct formation of the active center with respect to the counterpart. This interpretation of the findings would be in good agreement with the results demonstrating that the β_1 subunit lacking amino acids at position 204–303 (containing the NBS: amino acids positions 204–244) failed to show GC activity when co-expressed with the α_1 subunit, although this β_1 subunit exhibited the ability to bind to the α_1 subunit at reduced levels (Zhou *et al.*, 2004). In a recent study, it was reported that the N-terminal binding site of the bovine a_1 subunit (amino acid positions 61–128) plays a major role in heterodimerization (Wagner *et al.*, 2005). However, in this study, we did not observe such ability in the amino acids at positions 61–128. Here, we per-

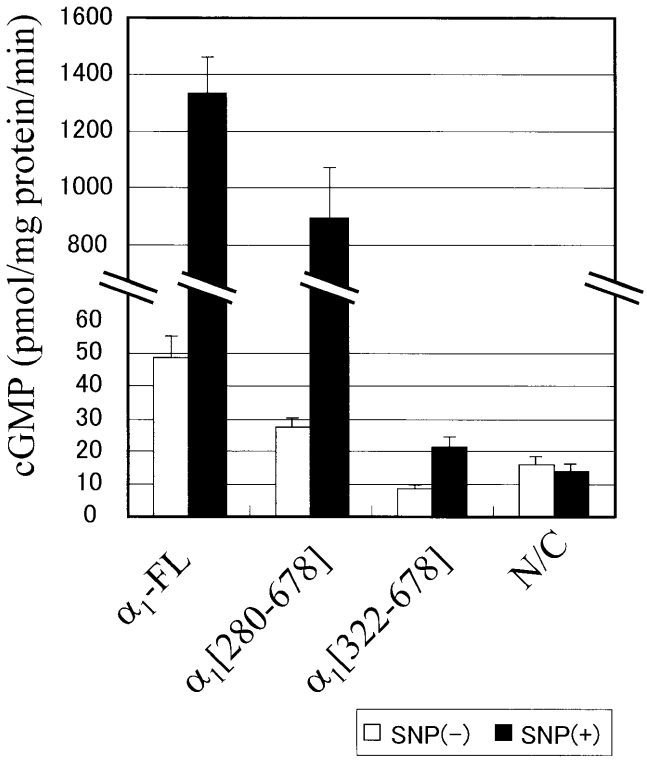

Fig. 3. The GC activity of N-terminal deletion mutant proteins. The GC activity in the lysates prepared from the respective infected Sf9 cells was assayed with (black columns) or without (white columns) SNP. The activity shown represents the means±S.E.M. obtained from three independent experiments.

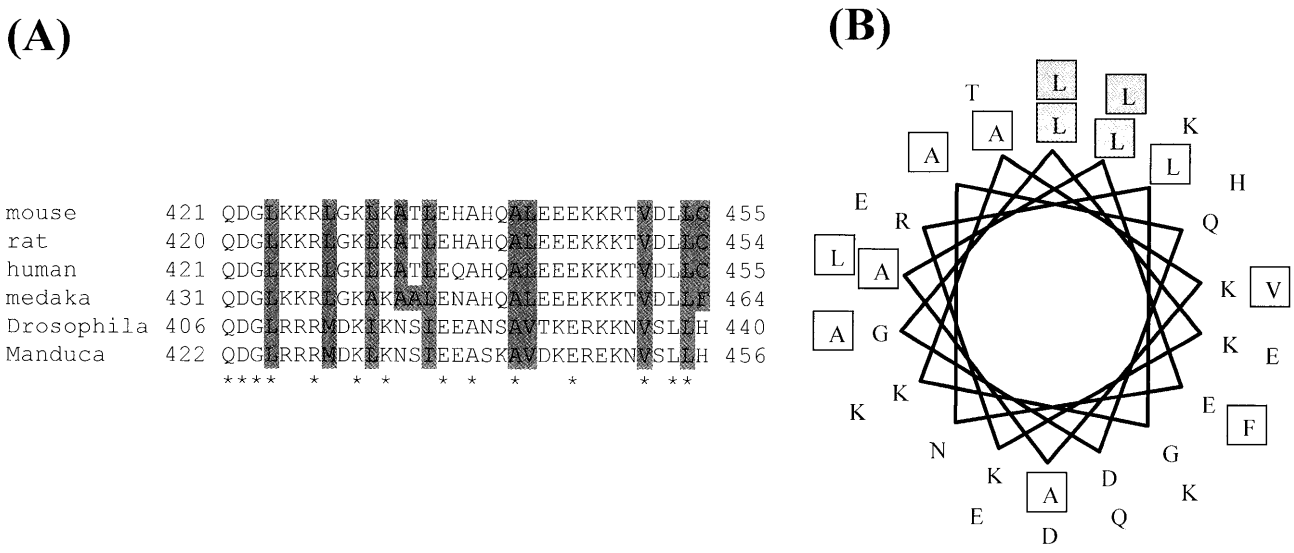

Fig. 4. The sequence and helical wheel diagram of the amphipathic α-helix of OlGCS-α_1. (A) The amino acid sequences of the putative amphipathic α-helices of various soluble GC-α_1 subunits were aligned. Identical residues are marked with asterisks, and the hydrophobic residues are darkened. The numbers denote the relative positions of the amino acids. (B) Hydrophobic amino acid residues are shown in boxes, and the Leu residues modified by site-directed mutagenesis are enclosed in shaded boxes.

formed both a pull-down assay and an assay to determine GC activity, and we demonstrated that OlGCS-α_1[280–678]$_{FLAG}$ was able to form a heterodimer with OlGCS-β_1-FL_{HT}.

Identification of amphipathic α-helix mediating heterodimerization between OlGCS-α_1 and OlGCS-β_1

To gain a better understanding of the nature of the CBS-like sequence of OlGCS-α_1 necessary for heterodimerization and GC activity, we predicted the secondary structure of OlGCS-α_1 using the PredictProtein server (http://www.embl-heidelberg.de/predictprotein/) and found that OlGCS-α_1[431-464] is able to form an amphipathic α-helix structure (Fig. 4). It has been reported that amphipathic α-helices often mediate protein-protein interactions (Carr *et al.*, 1991). Therefore, we investigated whether or not the amphipathic α-helix in the α_1 subunit was able to mediate the heterodimerization of both subunits of soluble GC after the introduction of a site-directed mutation to the α_1 subunit. To disturb the amphipathicity of the α-helix, we focused on the four Leu residues (Leu^{434}, Leu^{445}, Leu^{452}, and Leu^{463}) as shown in the shaded boxes in Fig. 4B; all of these Leu residues were predicted to be located exclusively on one side of the α-helix. Various site-directed mutant proteins were generated as described in Materials and Methods. According to the prediction of the secondary structure of the α_1 subunit that was carried out using the PredictProtein server, the α-helix structure was expected to be maintained, even after these four Leu residues were converted to Lys residues, thus leading to the loss of amphipathicity. *OlGCS-α_1-L434K$_{FLAG}$*, *L445K$_{FLAG}$*, *L463K$_{FLAG}$*, *L434, 445, 463K$_{FLAG}$*, or *L434, 445, 452, 463K$_{FLAG}$* was co-expressed with *OlGCS-β_1-FL$_{HT}$* in Sf9 cells, and the GC activity of each of the resulting cytosolic fractions was measured with or without SNP. As shown in Fig. 5, α_1-L434K$_{FLAG}$/β_1-FL_{HT} and α_1-L445K$_{FLAG}$/β_1-FL_{HT} showed almost the same basal and SNP-stimulated GC activities as those of α_1-FL_{FLAG}/β_1-FL_{HT}, but α_1- L463K$_{FLAG}$/β_1-FL_{HT}, L434, 445, 463K$_{FLAG}$/β_1-FL_{HT}, and L434, 445, 452, 463K$_{FLAG}$/β_1-FL_{HT} exhibited neither basal GC activity nor SNP-induced GC activity. To investigate the binding ability of each site-directed mutant protein to OlGCS-β_1-FL_{HT}, we performed a pull-down assay. As shown in Fig. 6, the binding ability of OlGCS-α_1-L434, 445, 463K$_{FLAG}$ and OlGCS-α_1-L434, 445, 452, 463K$_{FLAG}$ to OlGCS-β_1-FL_{HT} was remarkably reduced, although α_1-L434K$_{FLAG}$ and α_1-L445K$_{FLAG}$ both maintained their ability to bind to OlGCS-β_1-FL_{HT}. These results suggest that the amphipathicity in the putative α-helix region of OlGCS-α_1 is important for the formation of a heterodimer with OlGCS-β_1.

The amphipathicity of the α-helix in OlGCS-α_1[1-448]$_{FLAG}$ would be expected to be incomplete due to the lack of the C-terminal half of the putative amphipathic α-helix (see Fig. 1), which is likely to be a major reason for the inability of OlGCS-α_1[1–448]$_{FLAG}$ to bind to OlGCS-β_1. Surprisingly, OlGCS-α_1-L463K$_{FLAG}$ also maintained its binding ability to OlGCS-β_1-FL_{HT}, although the α_1-L463K$_{FLAG}$/β_1-FL_{HT} did not exhibit any GC activity, suggesting that the formation of a heterodimer of OlGCS-α_1 with OlGCS-β_1 is not sufficient for the enzyme GC activity, probably due to inadequate heterodimerization, which in turn would lead to the formation of an inadequate active center. As shown in Fig. 4A, Leu^{463} is conserved among the soluble GC-α_1 subunits of various species and is located in the C-terminal end of the amphipathic α-helix. In order to form an enzymatically active heterodimer, it appears to be essential that the active center is correctly formed between the catalytic domains of the α and β subunits. The conversion of Leu^{463} to Lys in OlGCS-α_1 might have led to the detachment of the hydrophobic bond at the C-terminal end of the amphipathic α-helix, although the remainder of the amphipathic α-helix maintained its hydrophobic bonds. The detachment of this region appears to lead to the formation of an incorrect active center between both domains of the catalytic subunits. This interpretation of the findings might account for why L463K$_{FLAG}$/β_1-FL_{HT} did not show any GC activity.

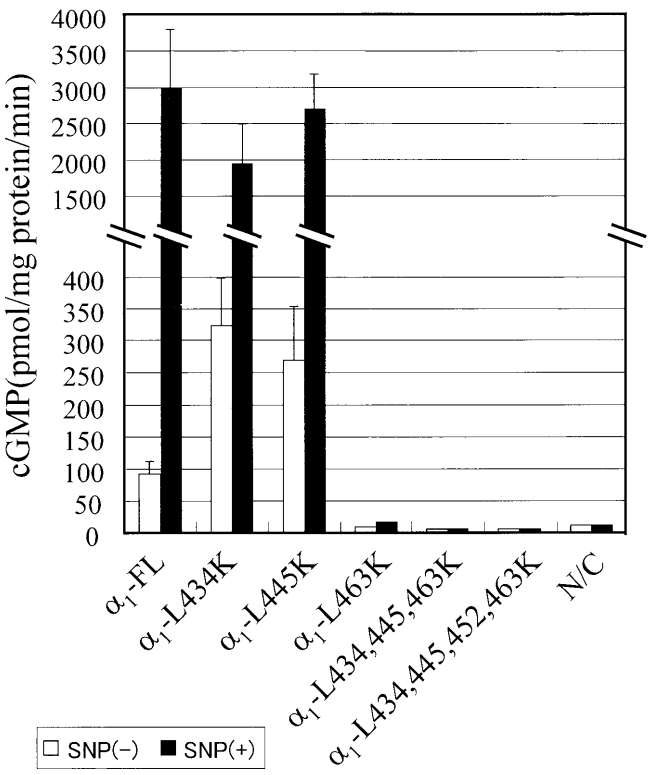

Fig. 5. The GC activity of site-directed mutant proteins. The GC activity in the lysates prepared from the respective infected Sf9 cells was assayed with (black columns) or without (white columns) SNP. The activity represents the means±S.E.M. obtained from three independent experiments.

As shown in Fig. 4A, the amino acid sequence in this region varies among the soluble GC-α_1 subunits of various species; changes in this amino acid sequence were not found to affect the formation of the putative amphipathic α-helix, suggesting that the amphipathic α-helix plays a critical role in the heterodimerization of the soluble GC α_1-subunit with the soluble GC-β_1 subunit. In addition, the analysis of

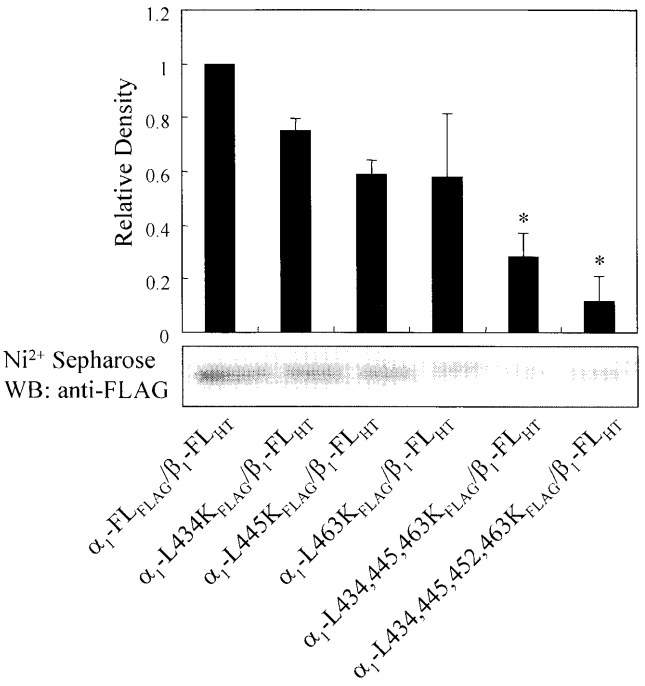

Fig. 6. Pull-down assay of site-directed mutant proteins. Sf9 cells were infected by baculovirus containing *OlGCS-α_1-FL_{FLAG}* or its site-directed mutants with *OlGCS-β_1-FL_{HT}*. The fractions exhibiting Ni^{2+} Sepharose-binding activity were analyzed by Western blotting with anti-FLAG antibody. The density of each band of the Ni^{2+} Sepharose-binding proteins reacted with anti-FLAG antibody was estimated using Scion imaging. The data are expressed by the fold density relative to the α_1-FL_{FLAG}/β_1-FL_{HT}, taken as , and the values shown represent the means±S.E.M. obtained from three independent experiments. *$P<0.05$ for the comparison with α_1-$L434K_{FLAG}$/β_1-FL_{HT} or α_1-$L445K_{FLAG}$/β_1-FL_{HT}.

the secondary structure of OlGCS-β_1 carried out with the PredictProtein server predicted that OlGCS-β_1[367–395] forms an amphipathic α-helix, and a similar analysis of OlGCS-α_2 also resulted in the prediction that OlGCS-α_2[535–555] forms an amphipathic α-helix. These results strongly suggest that the amphipathic α-helix mediates the heterodimerization of the soluble GC-α_1 subunit with soluble GC-β_1 subunits.

ACKNOWLEDGMENTS

We are grateful to the staff members at the Center for Advanced Science and Technology, Hokkaido University, for the use of their laboratory facilities. This study was supported by a Grant-in-Aid for Scientific Research from the Ministry of Education, Science, Sports, and Culture of Japan (no. 11236202) and by the National Project on Protein Structural and Functional Analyses.

REFERENCES

Carr DW, Stofko-Hahn RE, Fraser ID, Bishop SM, Acott TS, Brennan RG, Scott JD (1991) Interaction of the regulatory subunit (RII) of cAMP-dependent protein kinase with RII-anchoring proteins occurs through an amphipathic helix binding motif. J Biol Chem 266: 14188–14192

Chomczynski P, Sacchi N (1987) Single-step method of RNA isolation by acid guanidinium thiocyanate-phenol-chloroform extraction. Anal Biochem 162: 156–159

Drewett JG, Garbers DL (1994) The family of guanylyl cyclase receptors and their ligands. Endocr Rev 15: 135–162

Foerster J, Harteneck C, Malkewitz J, Schultz G, Koesling D (1996) A functional heme-binding site of soluble guanylyl cyclase requires intact N-termini of α_1 and β_1 subunits. Eur J Biochem 240: 380–386

Garbers DL, Koesling D, Schultz G (1994) Guanylyl cyclase receptors. Mol Biol Cell 5: 1–5

Garbers DL, Lowe DG (1994) Guanylyl cyclase receptors. J Biol Chem 269: 30741–30744

Gerzer R, Böhme E, Hofmann F, Schultz G (1981) Soluble guanylate cyclase purified from bovine lung contains heme and copper. FEBS Lett 132: 71–74

Harteneck C, Wedel B, Koesling D, Malkewitz J, Böhme E, Schultz G (1991) Molecular cloning and expression of a new alpha-subunit of soluble guanylyl cyclase. Interchangeability of the alpha-subunits of the enzyme. FEBS Lett 292: 217–222

Humbert P, Niroomand F, Fischer G, Mayer B, Koesling D, Hinsch KD, Gausepohl H, Frank R, Schultz G, Böhme E (1990) Purification of soluble guanylyl cyclase from bovine lung by a new immunoaffinity chromatographic method. Eur J Biochem 190: 273–278

Koesling D (1999) Studying the structure and regulation of soluble guanylyl cyclase. Methods 19: 485–493

Koesling D, Herz J, Gausepohl H, Niroomand F, Hinsch KD, Mulsch A, Böhme E, Schultz G, Frank R (1988) The primary structure of the 70 kDa subunit of bovine soluble guanylate cyclase. FEBS Lett 239: 29–34

Koglin M, Behrends S (2003) A functional domain of the a_1 subunit of soluble guanylyl cyclase is necessary for activation of the enzyme by nitric oxide and YC-1 but is not involved in heme binding. J Biol Chem 278: 12590–12597

Mikami T, Kusakabe T, Suzuki N (1998) Molecular cloning of cDNAs and expression of mRNAs encoding alpha and beta subunits of soluble guanylyl cyclase from medaka fish *Oryzias latipes*. Eur J Biochem 253: 42–48

Mikami T, Kusakabe T, Suzuki N (1999) Tandem organization of medaka fish soluble guanylyl cyclase α_1 and β_1 subunit genes. Implications for coordinated transcription of two subunit genes. J Biol Chem 274: 18567–18573

Russwurm M, Behrends S, Harteneck C, Koesling D (1998) Functional properties of a naturally occurring isoform of soluble guanylyl cyclase. Biochem J 335: 125–130

Sanger F, Nicklen S, Coulson AR (1992) DNA sequencing with chain-terminating inhibitors. 1977. Biotechnology 24: 104–108

Sawano A, Miyawaki A (2000) Directed evolution of green fluorescent protein by a new versatile PCR strategy for site-directed and semi-random mutagenesis. Nucleic Acids Res 28: E78

Stone JR, Marletta MA (1994) Soluble guanylate cyclase from bovine lung: activation with nitric oxide and carbon monoxide and spectral characterization of the ferrous and ferric state. Biochemistry 33: 5636–5640

Sunahara RK, Beuve A, Tesmer JJ, Sprang SR, Garbers DL, Gilman AG (1998) Exchange of substrate and inhibitor specificities between adenylyl and guanylyl cyclase. J Biol Chem 273: 16332–16338

Tesmer JJ, Sunahara RK, Gilman AG, Sprang SR (1997) Crystal structure of the catalytic domains of adenylyl cyclase in a complex with $G_{s\alpha}$ GTPγS. Science 278: 1907–1916

Tucker CL, Hurley JH, Miller TR, Hurley JB (1998) Two amino acid substitutions convert a guanylyl cyclase, Ret GC-1, into an adenylyl cyclase. Proc Natl Acad Sci USA 95: 5993–5997

Wagner C, Russwurm M, Jäger R, Friebe A, Koesling D (2005) Dimerizaion of NO-sensitive guanylyl cyclase requires the α_1 N

terminus. J Biol Chem 280: 17687–17693
Wedel B, Harteneck C, Foerster J, Friebe A, Schultz G, Koesling D (1995) Functional domains of soluble guanylyl cyclase. J Biol Chem 270: 24871–24875
Wedel B, Humbert P, Harteneck C, Foerster J, Malkewitz J, Böhme E, Schultz G, Koesling D (1994) Mutation of His-105 in the β_1 subunit yields a nitric oxide-insensitive form of soluble guanylyl cyclase. Proc Natl Acad Sci USA 91: 2592–2596
Wilson EM, Chinkers M (1995) Identification of sequences mediating guanylyl cyclase dimerization. Biochemistry 34: 4696–4701
Yao Y, Yamamoto T, Tsutsumi M, Matsuda M, Hori H, Naruse K, Mitani H, Shima A, Asakawa S, Shimizu N, Suzuki N (2003) Genomic structure and expression of the soluble guanylyl cyclase a_2 subunit gene in the medaka fish *Oryzias latipes*. Zool Sci 20: 1293–1304
Yuen PS, Potter LR, Garbers DL (1990) A new form of guanylyl cyclase is preferentially expressed in rat kidney. Biochemistry 29: 10872–10878
Zabel U, Hausler C, Weeger M, Schmidt HH (1999) Homodimerization of soluble guanylyl cyclase subunits. Dimerization analysis using a glutathione S-transferase affinity tag. J Biol Chem 274: 18149–18152
Zhang G, Liu Y, Ruoho AE, Hurley JH (1997) Structure of the adenylyl cyclase catalytic core. Nature 386: 247–253
Zhao Y, Schelvis JP, Babcock GT, Marletta MA (1998) Identification of histidine 105 in the b_1 subunit of soluble guanylate cyclase as the heme proximal ligand. Biochemistry 37: 4502–4509
Zhou Z, Gross S, Roussos C, Meurer S, Müller-Esterl W, Papapetropoulos A (2004) Structural and functional characterization of the dimerization region of soluble guanylyl cyclase. J Biol Chem 279: 24935–24943

(Received March 30, 2005 / Accepted June 17, 2005)